Laser beams under tight focusing conditions and electron charge diagnostics in a laser-plasma environment

David Gregocki

david.gregocki@ino.cnr.it

Consiglio Nazionale delle Ricerche (CNR), Istituto Nazionale di Ottica, Pisa, Italy
Dipartimento di Fisica, Università di Pisa, Pisa, Italy

Table of contents

2 - Laser beams under tight focusing conditions

1.1 Motivation:

- Off-Axis Parabolic (**OAP**) mirrors are an important element in many high-power laser facilities
- Able to **focus laser pulses** to relativistic intensities $\gtrsim 10^{18}$W/cm^2
    - Enabling new studies in laser-matter interactions
- However, **unexpected field distortions** can seriously impact the interaction and results
    - Hamper reaching maximum intensity in the focus
    - Limit the efficiency
    - Impact the particle pointing direction in laser particle acceleration
- These distortions are **more pronounced under** tight focusing conditions (**f/#<1**)
- Therefore, the exact **knowledge of focused** electromagnetic **fields is essential**

2 - Laser beams under tight focusing conditions

1.2 Theoretical layout:

- The OAP surface can be defined by the following equations

$$z = \frac{(x^2 + y^2)}{4 f_p}, \qquad (x - d_{\mathrm{OAD}})^2 + y^2 \leq \left(\frac{D}{2}\right)^2,$$

where D is the OAP diameter. Based on the geometry

$$f = \sqrt{(f_p - a d_{\mathrm{OAD}}^2)^2 + d_{\mathrm{OAD}}^2},$$

$$\tan(\theta_{\mathrm{OA}}) = \frac{d_{\mathrm{OAD}}}{f_p - a d_{\mathrm{OAD}}^2} \quad \wedge \quad f = \frac{d_{\mathrm{OAD}}}{\sin(\theta_{\mathrm{OA}})}.$$

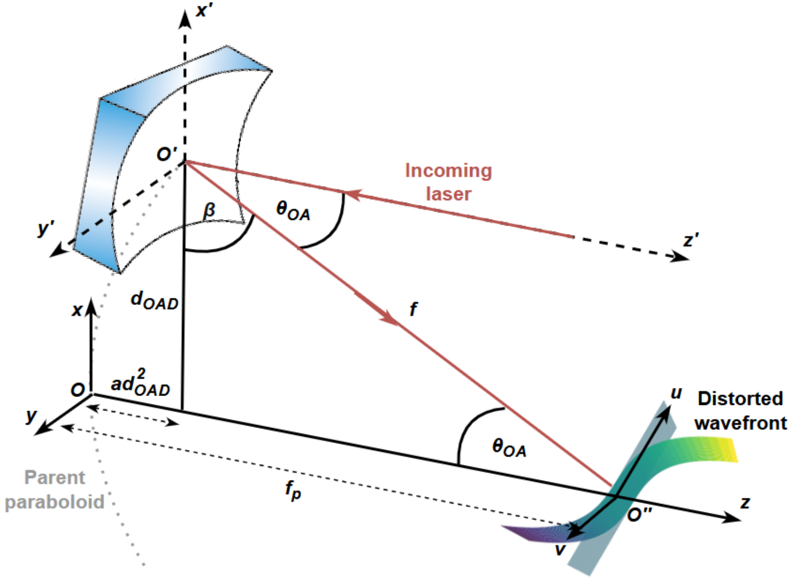

2 - Laser beams under tight focusing conditions

J. A. Stratton and L. J. Chu, Phys. Rev. 56, 99-107 (1939)
L. Labate, High Power Laser Sci. Eng. 6, e32 (2018)
L. Labate, Appl. Opt. 55, 6506-6515 (2016)

1.2 Theoretical layout:

- Based on the Stratton-Chu theory, if the electric and magnetic fields are known on a closed surface A, then the diffracted fields at a point x_p in the far-field are defined as

$$\mathbf{E}(\mathbf{x}_p) = \frac{1}{4\pi}\int_A [\mathrm{i}k(\hat{\mathbf{n}}\times\mathbf{B})G + (\hat{\mathbf{n}}\times\mathbf{E})\times\nabla G + (\hat{\mathbf{n}}\cdot\mathbf{E})\nabla G]\mathrm{d}A$$
$$\mathbf{B}(\mathbf{x}_p) = \frac{1}{4\pi}\int_A [\mathrm{i}k(\mathbf{E}\times\hat{\mathbf{n}})G + (\hat{\mathbf{n}}\times\mathbf{B})\times\nabla G + (\hat{\mathbf{n}}\cdot\mathbf{B})\nabla G]\mathrm{d}A,$$

where k is the angular wavenumber of the incident pulse, G is the Green function

$$G(\mathbf{x}) = G(\mathbf{x}-\mathbf{x}_p) = \frac{\mathrm{e}^{\mathrm{i}k|\mathbf{x}-\mathbf{x}_p|}}{|\mathbf{x}-\mathbf{x}_p|} \equiv \frac{\mathrm{e}^{\mathrm{i}ku}}{u} \quad \wedge \quad \nabla G(\mathbf{x}) = ik\left(1-\frac{1}{iku}\right)\frac{G(\mathbf{u})}{u}\mathbf{u}, \quad \text{where} \quad \mathbf{u} = \mathbf{x}-\mathbf{x}_p \quad \text{and} \quad u = |\mathbf{u}|$$

and the area element $\mathrm{d}A$ and the normal to the surface $\hat{n}$ are defined as

$$dA = \sqrt{1+s(x,y)}\,dxdy, \qquad \hat{\mathbf{n}} = \frac{1}{\sqrt{1+s(x,y)}}\begin{pmatrix} -x/2f \\ -y/2f \\ 1 \end{pmatrix} \qquad \text{where} \qquad s(x,y) = (x^2+y^2)/4f^2$$

2 - Laser beams under tight focusing conditions

1.2 Theoretical layout:

Considering a 100% reflection, the fields appearing in the Stratton-Chu theory can be written as a function of the incident fields

$$\mathbf{E}(\mathbf{x}) = 2\hat{\mathbf{n}}(\hat{\mathbf{n}} \cdot \mathbf{E}_{\mathrm{Inc}}(\mathbf{x})), \quad \mathbf{B}(\mathbf{x}) = 2\mathbf{B}_{\mathrm{Inc}}(\mathbf{x}) - 2\hat{\mathbf{n}}(\hat{\mathbf{n}} \cdot \mathbf{B}_{\mathrm{Inc}}(\mathbf{x}))$$

thus for the electric field at x_p in the far-field applies

$$\mathbf{E}(\mathbf{x}_p) = \frac{1}{2\pi}\int_{\mathrm{OAP}} \left[ik(\hat{\mathbf{n}} \times \mathbf{B}_{\mathrm{Inc}})G + (\hat{\mathbf{n}} \cdot \mathbf{E}_{\mathrm{Inc}})\nabla G\right] dA$$

The incident electric field, can be expressed as

$$\mathbf{E}_{\mathrm{Inc}}(\mathbf{x}) = A(x,y)\left(\cos(\delta)\widehat{\mathbf{e}_{\mathbf{x}}} + \sin(\delta)\widehat{\mathbf{e}_{\mathbf{y}}}\right) e^{ikp(\mathbf{x})}$$

where

$$A(x,y) = A_0 \exp\left\{-\frac{1}{2}\left[\left(\frac{x-d_{\mathrm{OAD}}}{\sigma_x}\right)^2 + \left(\frac{y}{\sigma_y}\right)^2\right]^n\right\} \quad \text{and} \quad p(\mathbf{x}) = a\left(d_{\mathrm{OAD}}^2 - (x^2+y^2)\right)$$

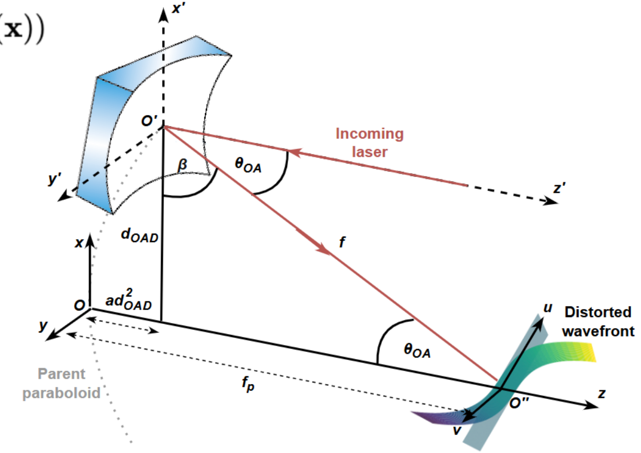

2 - Laser beams under tight focusing conditions

1.2 Theoretical layout:

Eventually

$$E_j^{\mathrm{Re}}(\mathbf{x_p},t) = -\frac{1}{\lambda}\int_{\mathrm{OAP}} A(x,y)\times\left[\mathfrak{Im}\left\{g^{(E_j)}\right\}\cos\left(kv-\omega t\right)+\mathfrak{Re}\left\{g^{(E_j)}\right\}\sin\left(kv-\omega t\right)\right]\mathrm{d}x\mathrm{d}y$$

$$E_j^{\mathrm{Im}}(\mathbf{x_p},t) = -\frac{1}{\lambda}\int_{\mathrm{OAP}} A(x,y)\times\left[\mathfrak{Im}\left\{g^{(E_j)}\right\}\sin\left(kv-\omega t\right)-\mathfrak{Re}\left\{g^{(E_j)}\right\}\cos\left(kv-\omega t\right)\right]\mathrm{d}x\mathrm{d}y$$

where

$$g^{(E_x)} = \frac{1}{u}\cos\delta-\left(1-\frac{1}{iku}\right)\frac{1}{u^2}\times\left(\frac{x}{2f_p}\cos\delta+\frac{y}{2f_p}\sin\delta\right)(x-x_p)\,,$$

$$g^{(E_y)} = \frac{1}{u}\sin\delta-\left(1-\frac{1}{iku}\right)\frac{1}{u^2}\times\left(\frac{x}{2f_p}\cos\delta+\frac{y}{2f_p}\sin\delta\right)(y-y_p)\,,$$

$$g^{(E_z)} = \frac{1}{u}\left(\frac{x}{2f_p}\cos\delta+\frac{y}{2f_p}\sin\delta\right)-\left(1-\frac{1}{iku}\right)\frac{1}{u^2}\times\left(\frac{x}{2f_p}\cos\delta+\frac{y}{2f_p}\sin\delta\right)(z-z_p)\,,$$

and

$$v(\mathbf{x},\mathbf{x}_p) = u(\mathbf{x},\mathbf{x}_p)+p(\mathbf{x}_p)$$

2 - Laser beams under tight focusing conditions

1.3 Results:

- Wavefront distortions can be studied from a weighted average of the angles θ weighted by the pulse intensity I

$$\bar{\theta} = \frac{\sum_i \theta_i I_i}{\sum_j I_j} \qquad \text{where} \qquad \theta = \arccos\left(\frac{|k_z|}{|\mathbf{k}|}\right)$$

- To obtain a rule of thumb in predicting $\bar{\theta}$ for a given OAP configuration

$$\bar{\theta}(f/\#A, B) = A \cdot (f/\#)^B = \frac{\theta_{OA}}{20.7} f/\#^{-1.9}$$

$\bar{\theta}$ approximation			
θ_{OA} [°]	A [±0.01°]	B ±0.01	χ^2 ± 0.09
6	0.27	-1.93	0.43
12	0.55	-1.91	0.60
24	1.10	-1.88	1.05
30	1.38	-1.86	1.28
45	2.12	-1.83	1.74
60	2.92	-1.81	1.94
78	4.06	-1.82	1.62
90	5.00	-1.85	0.98

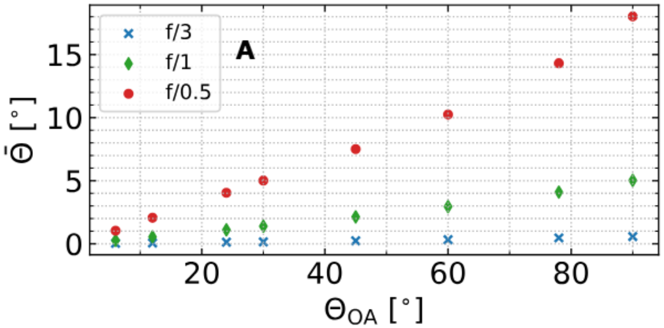

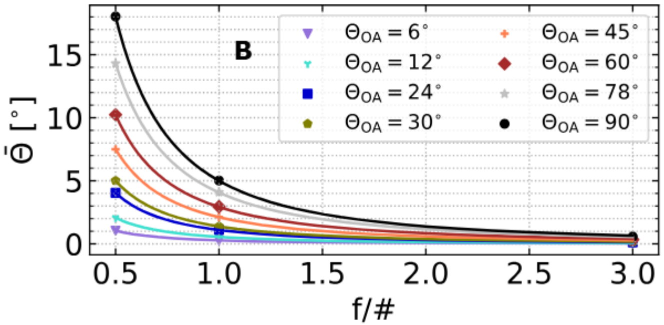

2 - Laser beams under tight focusing conditions

1.3 Results:

- So far, only a monochromatic laser pulse has been considered. However, electric fields of non-monochromatic laser can be described as

$$\tilde{E}_j = \sum_{\lambda} \sqrt{\exp\left(-\frac{(\lambda-\lambda_0)^2}{2\sigma_\lambda^2}\right)}\left(E_j^{\mathrm{Re}} + iE_j^{\mathrm{Im}}\right)$$

where λ_0 is the central wavelength. Considering λ_0=800 nm, $\lambda \in < 780{,}820 >$, $\sigma_\lambda = 15$ nm

- The dependence of $\bar{\theta}$ on θ_{OA} can be compared between mono- and non-monochromatic pulses. In addition, different time periods within the optical cycle of laser can be considered

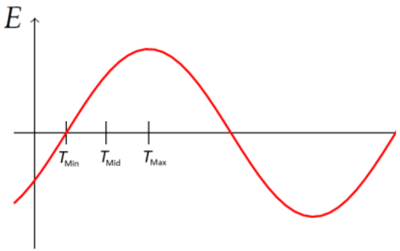

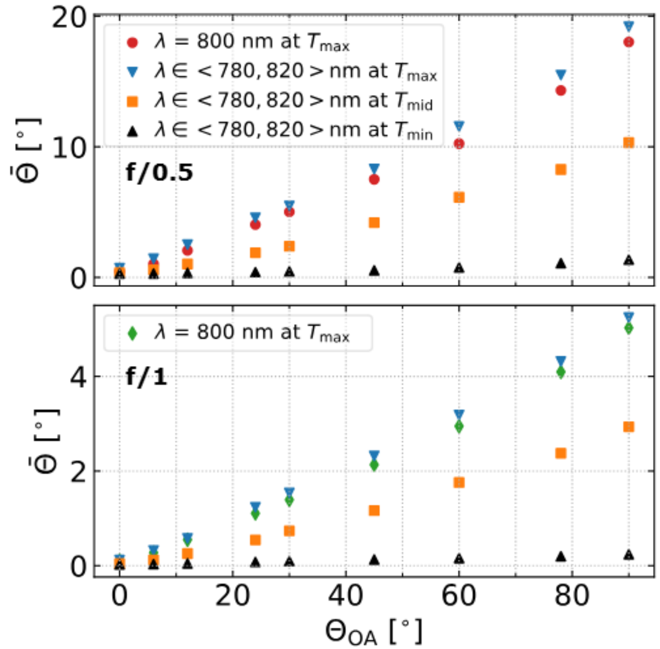

2 - Laser beams under tight focusing conditions

1.3 Results:

Monochromatic laser with different λ_0

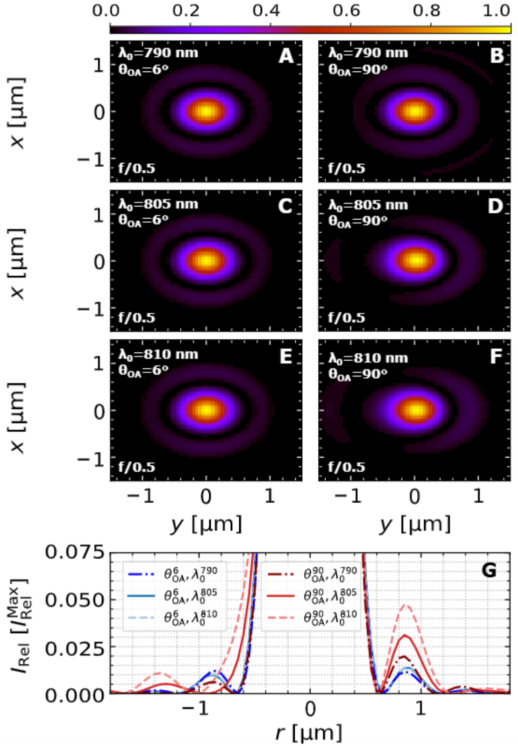

Non-monochromatic laser

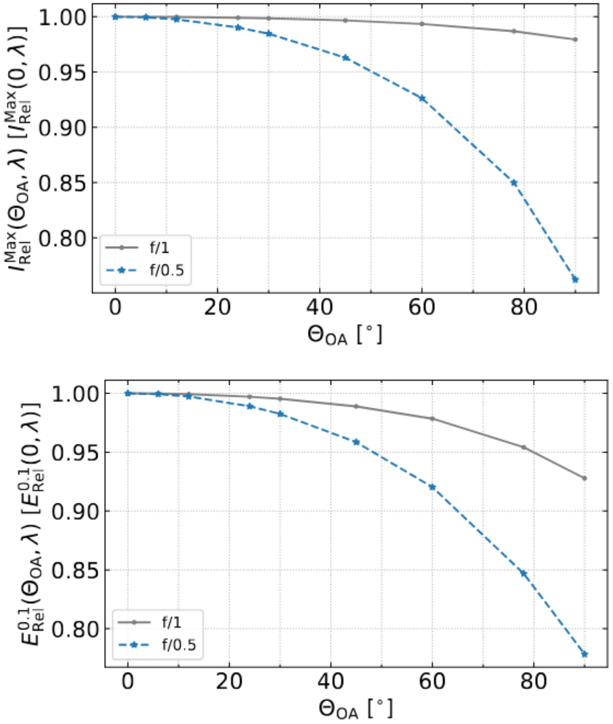

01 – Summary I. part

- Off-axis parabolic mirrors are widely used in many high-power laser facilities due to their ability to focus laser pulses to relativistic intensities
- By employing the full Stratton-Chu vector diffraction theory, field distortion effects related to the use of an OAP mirror under tight focusing conditions
- The results point to the distortions in the initially planar laser wavefront. Such distortions are most dominant for increasing off-axis angles.
- Consequently, the relative laser peak intensity and relative energy losses were observed for f/1 and f/0.5 OAP mirrors

2 - Electron charge diagnostics in a laser-plasma environment

2.1 Motivation:

- Integrating current transformers (**ICT**) have been used as reliable charge diagnostics in the radio-frequency acceleration's community
- Quickly gained popularity also in laser-plasma acceleration (LPA) field thanks to **nondestructive, energy independent** (and compact) **charge measurement**
  - **However,** in some cases
    - ICT measurements **overestimated charge** by more than an order of magnitude[1].
    - ICT measurements **overestimated charge** by 3-4 times[2].
    - Charge measurement **consistent with calibration** – Measurement at large distance (**4m**) from interaction region[3].
  - Main **unwanted contributor** to charge overestimation **was** electro-magnetic pulse (**EMP**) **signal**
    - Can we correlate ICT charge and Lanex screen emission signal?
    - Is EMP influence observed also in our case?

[1] *Glinec et al., Rev. Sci. Instrum. 77, 103301 (2006)*
[2] *B. Hidding et al., Rev. Sci. Instrum. 78, 083301 (2007)*
[3] *K. Nakamura et al., PRST-AB 14, 062801 (2011)*

2 - Electron charge diagnostics in a laser-plasma environment

2.2 General description:

- **I**ntegrating **C**urrent **T**ransformer is a capacitively shorted transformer and a fast read out transformer in a common magnetic circuit
- ICT consists of a coil with magnetic core shaped into a loop through which electron bunches can pass
- Able to bypass low-frequency components while allowing high-frequency signals to pass through = rapid signal transfer
- Core material of high permeability = low hysteresis losses and quick responds
- It is a passive transformer, and the signal is processed/integrated by the ICT controller

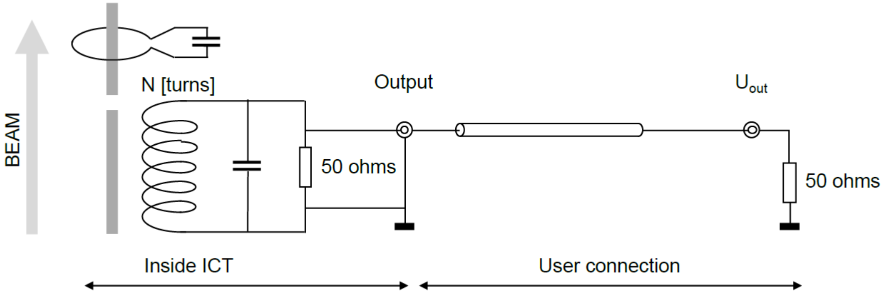

ICT

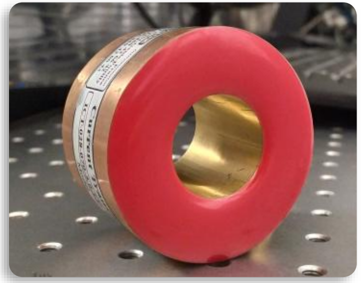

2 - Electron charge diagnostics in a laser-plasma environment

2.2 General description:

Integrating Op-Amp (ideal case)

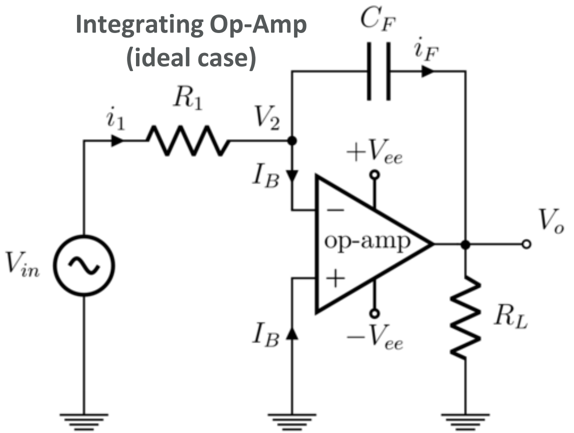

- Electron charge induces a voltage in the coil
- Integrating over this voltage produces an output voltage proportional to the electron beam charge
- Integration is ensured by the integrating operational amplifier (Op-Amps) found in the ICT controller

From Kirchhoff's current law:

$i_1 = I_B + i_F$ where $I_B = 0$ for ideal Op-Amp

Using the capacitor current equation

$$i_F = C_F \frac{\mathrm{d}(V_2 - V_0)}{\mathrm{d}t}$$

and rewriting i_1

$$i_1 = \frac{V_{\text{in}} - V_2}{R_1}$$

$$\frac{V_{\text{in}} - V_2}{R_1} = C_F \frac{\mathrm{d}(V_2 - V_0)}{\mathrm{d}t}$$ where $V_2 = 0$ for ideal case

$$\frac{V_{\text{in}}}{R_1} = -C_F \frac{\mathrm{d}V_0}{\mathrm{d}t} \quad \Big/ \int_0^t$$

$$\int_0^t \frac{V_{\text{in}}}{R_1}\mathrm{d}t = -\int_0^t C_F \frac{\mathrm{d}V_0}{\mathrm{d}t}\mathrm{d}t$$ if $V_0 = 0$ for $t = 0$

$$V_0 = -\frac{1}{R_1 C_F}\int_0^t V_{\text{in}}\mathrm{d}t$$

2 - Electron charge diagnostics in a laser-plasma environment

2.2 General description:

- One window integrates the signal, and the second one integrates the background for noise reduction

Ideal signal for integration (Example)

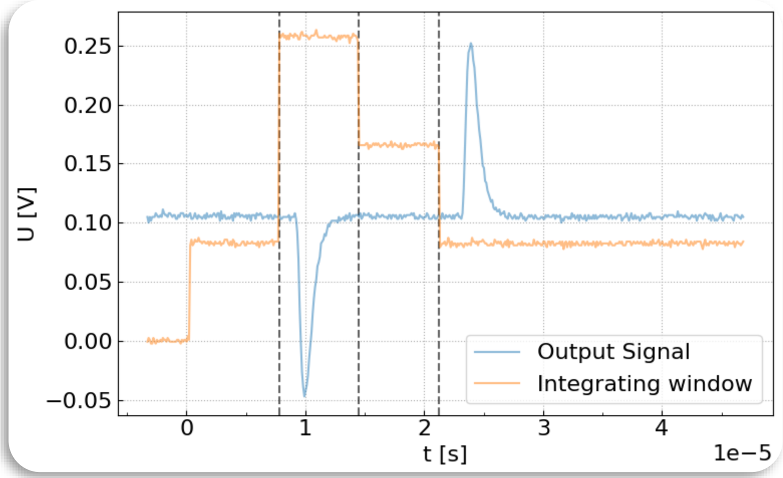

Signal from LPA generated electrons

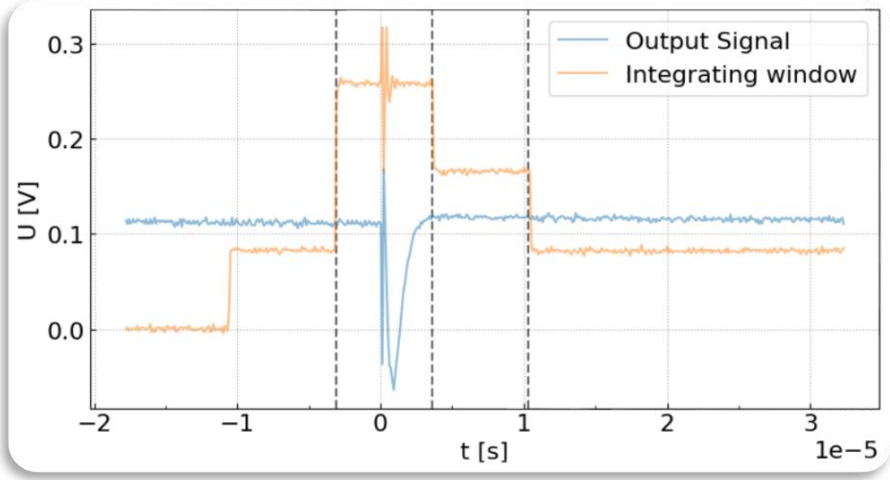

2 - Electron charge diagnostics in a laser-plasma environment

2.2 General description:

- One window integrates the signal, and the second one integrates the background for noise reduction

Ideal signal for integration (Example)

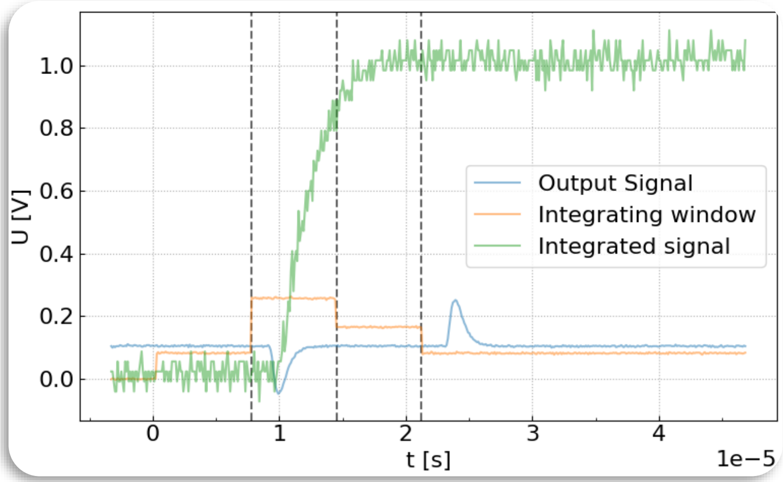

Signal from LPA generated electrons

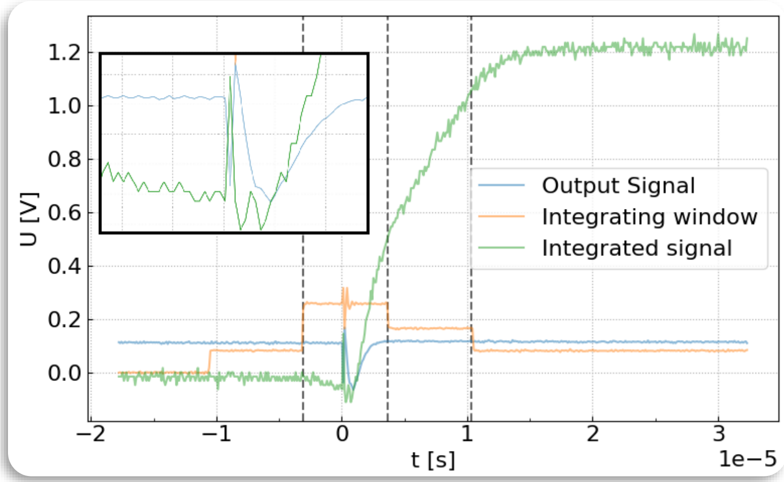

2 - Electron charge diagnostics in a laser-plasma environment

2.3 Experimental setup:

1
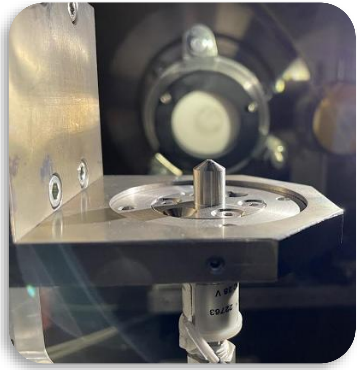

2
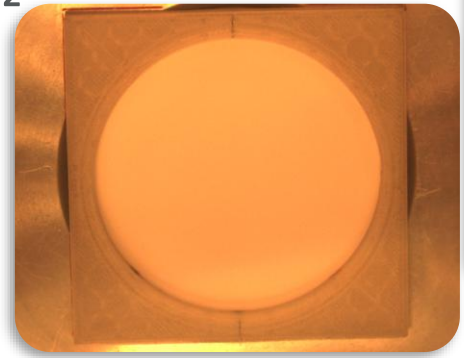

3
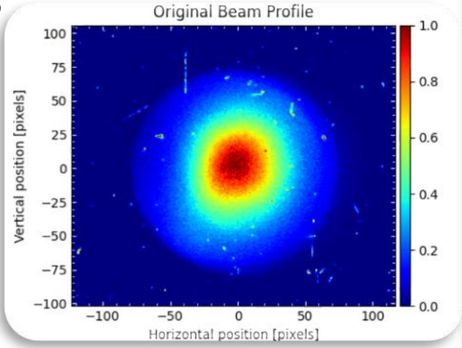

4
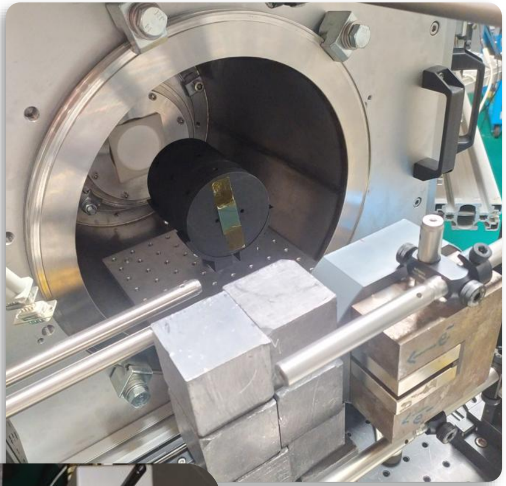

5
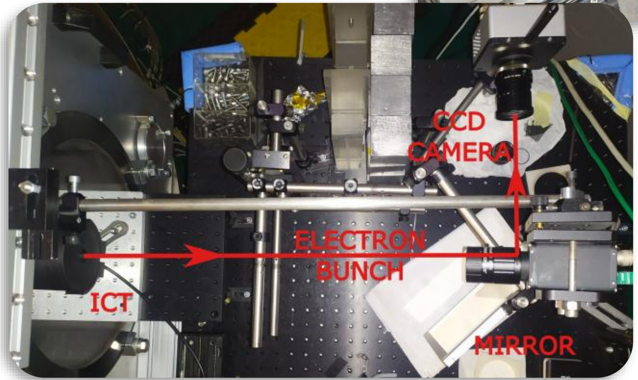

- LPA generated electrons passed through the Lanex screen after the vacuum-air transition
- Later, they passed through the ICT and RCF (EBT3)
- Afterwards, magnetic spectrometer was placed to measure the electron energy

2 - Electron charge diagnostics in a laser-plasma environment

2.3 Experimental setup:

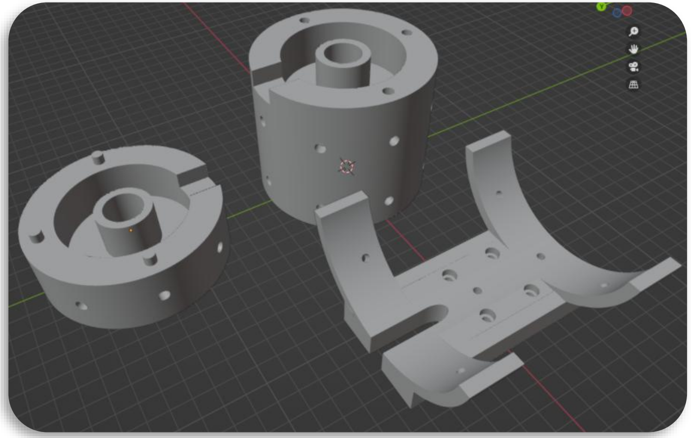

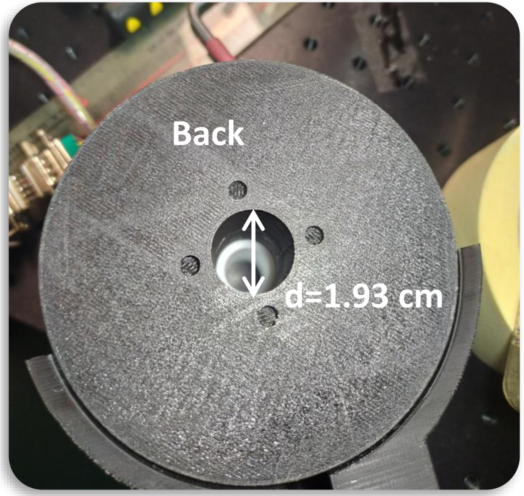

- ICT mount/shielding was designed in Blender
- 3D printed with PLA filament
- The front part allows the collimator to be replaced
- CMC filter – ferrite magnet was attached close to the ICT
- Double shielded and grounded BNC cable was used

2 - Electron charge diagnostics in a laser-plasma environment

2.4 Results:

1. Step: Retrieve the charge from the ICT

Shot no.	Q_{ICT} [±5 pC] RCF 1	RCF 2	RCF 3	RCF 4
1	78.6	56.3	87.3	117.8
2	67.9	90.8	82.5	99.9
3	101.3	55.4	40.4	93.2
4	62.2	42.6	83.3	98.3
5	30.1	82.4	76.2	120.3
6	59.0	113.7	111.8	103.4
7	73.6	76.7	83.0	56.8
8	53.6	83.7	80.5	135.2
9	91.0	91.3	84.9	103.6
10	56.3	59.2	113.4	111.8
Average:	67.4±19.2	75.2±20.4	84.3±19.0	104.0±19.7
Sum:	673.6±15.8	752.1±15.8	843.3±15.8	1040.3±15.8
Dose:	0.158±0.007	0.186±0.009	0.201±0.010	0.249±0.011

2. Step: Calculate the charge from the dose on the RCF and compare it

- **Dose-Fluence equation:**

$$D = K \sum_i \left(\frac{S}{\rho}\right)_i \phi_i^{RCF} \quad \text{where} \quad \phi_{Total}^{RCF} = \sum_i \phi_i^{RCF}$$

where $K = 1.6 \cdot 10^{-10}$, $\left(\frac{S}{\rho}\right)_i$ is the collision stopping power, and index i is the i-th energy bin index

- **Fluence-Charge equation:**

$$Q^{RCF} = \phi_{Total}^{RCF} \cdot \left(\frac{d}{2}\right)^2 \pi \cdot e$$

- However, the first equation represents undetermined system and additional assumptions needs to be made

2 - Electron charge diagnostics in a laser-plasma environment

2.4 Results:

- For the electron energy measured, $\left(\frac{S}{\rho}\right)_i$ changes only at the third decimal place
  - Thus, a weighted average can be assumed instead

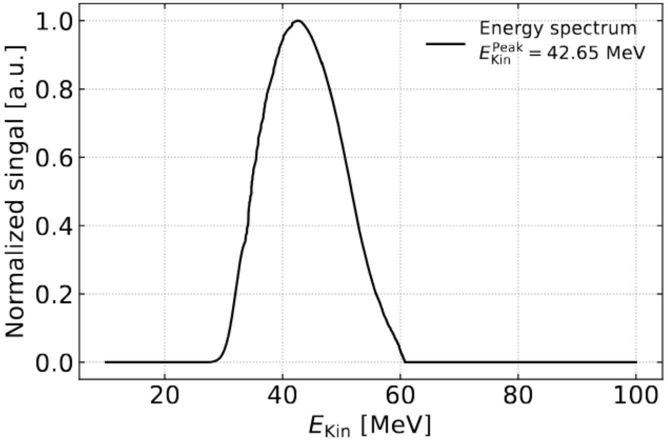

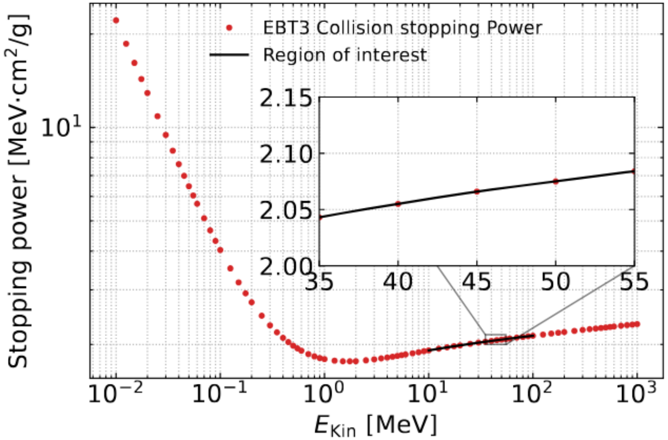

$$\overline{\left(\frac{S}{\rho}\right)} = \sum_j w_j \left(\frac{S}{\rho}\right)_i$$

where

$$w_j = \frac{y_j}{\sum y}$$

y_j is the magnitude of the j-the energy bin

- Given the electron energy, a fraction of electrons will be lost and won't deposit a dose to the RCF. Thus, additional simulations are necessary.

2 - Electron charge diagnostics in a laser-plasma environment

2.4 Results:

- Monte-Carlo simulations to determine a fraction of lost electrons
  - Lost between the ICT and RCF

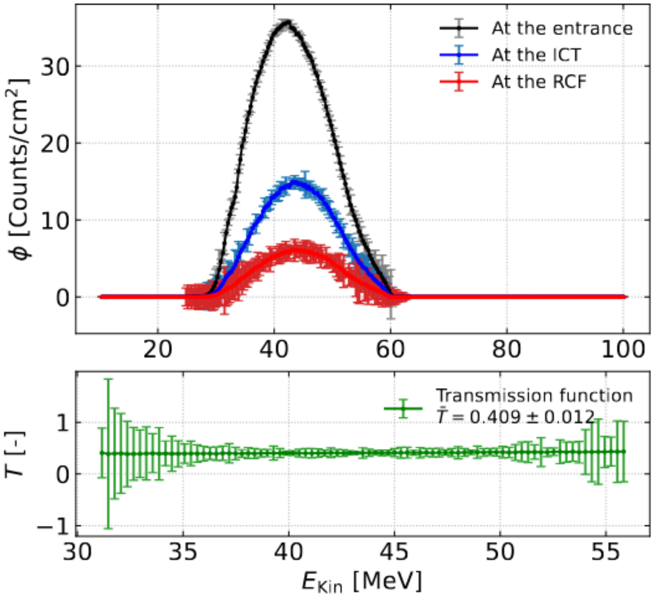

- Therefore, $\phi_{Total}^{RCF} = \sum_i \phi_i^{RCF} = \sum_i T_i \phi_i^{ICT}$. Since T_i can be assumed as constant $\forall i$, an average $\bar{T}$ can be considered further
- The Dose-Fluence equation can be simplified

$$D = K \cdot \overline{\left(\frac{S}{\rho}\right)} \cdot \bar{T} \sum_i \phi_i^{ICT}$$

- Now, ϕ_{Total}^{ICT} can be expressed and put into the fluence-charge equation

	Q_{RCF} [pC]			
	RCF 1	RCF 2	RCF 3	RCF 4
Single Shot:	54.9±24.3	64.6±31.3	69.9±34.8	86.5±38.2

Summary II. part

- *Ultrashort and ultraintense laser pulses can be used to accelerate electrons up to relativistic energies*
- *ICTs provide noninvasive, energy-independent charge monitoring*
- *In laser-plasma acceleration, electromagnetic signals can influence ICT measurements*
- *However, with proper ICT shielding and its placement, the overestimation from EMPs can be eliminated*

01 - Intense Laser Irradiation Laboratory Overview

Scientific staff:

Leonida A. **GIZZI*** (Head of lab)
Fernando **BRANDI**
Gabriele **CRISTOFORETTI**
Petra **KOESTER**
Luca **LABATE***
Federica **BAFFIGI**
Lorenzo **FULGENTINI**
Alessandro **FREGOSI** term
Daniele **PALLA** term
Costanza **PANAINO** term
Simona **PICCININI** term
Martina **SALVADORI** term
Emma **HUME** postdoc
Federico **AVELLA** PhD student
David **GREGOCKI** PhD student
Simon **VLACHOS** PhD student
Gianluca **CELLAMARE** (associated)

Antonio **GIULIETTI** associated
**Also at Istituto Nazionale di Fisica Nucleare*

EuPRAXIA Doctoral Network

Acknowledgement:

This project has received funding from the European Union MSCA network "EuPRAXIA-DN" (grant agreement no. 101073480) and the UKRI guarantee funds. The authors ackowledge the following contributions: EU Horizon 2020 Research and Innovation Program EuPRAXIA Preparatory Phase, under Grant Agreement No. 101079773 and IFAST, under Grant Agreement No. 101004730. This research has been co-funded by the European Union - NextGeneration EU ``Integrated infrastructure initiative in Photonic and Quantum Sciences'' - I-PHOQS (IR0000016, ID D2B8D520, CUP B53C22001750006) and ``EuPRAXIA Advanced Photon Sources'' - EuAPS (IR0000030, CUP I93C21000160006).

Thank you!

david.gregocki@ino.cnr.it